Energy & Environmental Science

Addressing Global Water Stress Using Desalination and Atmospheric Water Harvesting: A Thermodynamic and Technoeconomic Perspective

Journal:	*Energy & Environmental Science*
Manuscript ID	EE-PER-09-2023-002916
Article Type:	Perspective
Date Submitted by the Author:	01-Sep-2023
Complete List of Authors:	Kocher, Jordan; Georgia Institute of Technology, Mechanical Engineering Menon, Akanksha; Georgia Institute of Technology, Mechanical Engineering

Broader context statement:

Freshwater constitutes only 3% of the available water on Earth, and it is a critical resource for various sectors of the economy ranging from energy production to agriculture. Rapid population growth and climate change are depleting this finite resource, which is projected to result in severe water stress across the globe. To combat this, methods of artificially producing freshwater must be implemented. One such well-established technology is desalination, in which fresh water is extracted from saline water (typically seawater) in large, centralized treatment facilities located at the coast. With over 60% of the global population living in inland regions, this desalinated water must also be transported (using a combination of pipes, canals, and tunnels), which increases the cost of the water and the energy consumed. In contrast, atmospheric water harvesting (AWH) is an emerging technology that has garnered significant attention for decentralized freshwater production by extracting moisture from air and condensing it into liquid water. While AWH is often claimed to be low cost, there is no data to support this and a direct comparison to desalination on the common basis of energy consumption and lifetime costs is missing. This work provides a comprehensive thermo-economic analysis of these different technologies while taking into consideration population density, weather, and water risk data to address global freshwater availability. This approach reveals the significant advantage of desalination, but also pinpoints a niche and provides guidance for the development of efficient and low cost AWH.

ARTICLE Energy & Environmental Science

Addressing Global Water Stress using Desalination and Atmospheric Water Harvesting: A Thermodynamic and Technoeconomic Perspective

Received 00th January 20xx,
Accepted 00th January 20xx

DOI: 10.1039/x0xx00000x

Jordan D. Kocher [a] and Akanksha K. Menon*[a]

Freshwater is a critical resource but excessive withdrawal of natural reserves and inefficient water management, as well as climate change and pollution have resulted in global water stress that is projected to impact 4 billion people by 2030. Methods of artificially producing freshwater include desalination, which is a well-established process in which water is extracted from a saline source (typically seawater). Atmospheric water harvesting (AWH) is an alternate emerging process in which water vapor is extracted from ambient air and condensed into freshwater. Although AWH has attracted attention for decentralized water production using different materials and technologies (*e.g.,* sorbents, active, or passive cooling), the energy consumption and costs associated with practical systems with meaningful water yields to address water stress has not been reported. Herein we present a thermodynamic and technoeconomic framework to evaluate different AWH systems on the basis of these performance metrics (kWh/m^3 and \$/m^3), and we compare it to desalination at the coast with clean water transport inland (distributed). These results are weighted by the population and water risk across all global locations to identify regions where each process may be viable. We find that AWH is more energy intensive for 84% of the global population even if it operates reversibly (impractical system) when compared to distributed seawater desalination. Furthermore, a practical AWH system has a minimum levelized cost of water (LCOW) of \$10/m^3, which is significantly higher than seawater desalination even after accounting for water transport costs. The analysis reveals a niche where AWH can be the lowest cost option, *i.e.,* water harvesting in arid locations far from the coast (*e.g.,* Sahara Desert) using sorbents, although this represents only a small fraction of the water-stressed population. Ultimately, this analysis framework informs material and system design targets for AWH research and development to maximize global impact.

Introduction

The increasing demand for clean water has resulted in global water crises[1,2], with over 2 billion people living in water stressed countries[3]. Climate change, population growth, and economic activities (agriculture, power generation, etc.) have exacerbated water scarcity by depleting natural freshwater reserves[2,4,5], thus necessitating the use of cost-effective methods for artificially producing clean water. Seawater desalination[6,7] is a well-established process for separating salts from water that has been deployed at scale in many coastal locations. The current global desalination capacity is approximately 95 million m^3/day, with 40% of this capacity located in the Middle East[8]. In fact, many Gulf countries satisfy more than half of their potable water demand using large desalination plants[9–12]. This is because seawater desalination is economically viable for coastal regions, due to the abundance of a saline water source and discharge of brine into the ocean. However, over 60% of the global population is located in inland regions[13], which requires transporting the desalinated water[14]. For example, drought-prone and arid regions around the globe (*e.g.,* Phoenix, Arizona[15] and South Australia[16]) are pursuing this distributed desalination approach, with recent approvals to construct a coastal desalination plant and a 200-mile water conveyance pipeline inland. Desalination of inland saline sources (*e.g.*, brackish groundwater, industrial discharges, etc.[17–20]) has emerged as another option for distributed freshwater production[21,22] but its applicability has thus far been limited by the source (which can be geographically widespread and of varying salinity), as well as challenges with brine management[21].

Atmospheric water harvesting[23–31] (AWH) is another process for producing freshwater that has recently received great interest. In AWH, water vapor is extracted from ambient air and condensed into liquid water. Active dew harvesting AWH devices (driven by refrigeration) are commercially available for potable water production but are energy intensive (~3 kWh/L), while sorbents and radiative cooling surfaces that can passively harvest water from air are being developed by researchers. Some of these sorbents can harvest moisture from relative humidities as low as 12%[30], but device demonstrations have primarily been at small scales. For example, LaPotin *et al.* demonstrated a sorbent-based AWH device that harvested ~0.8 L/m^2/day[31], while Haechler *et al*. designed a radiative cooling surface that achieved peak water harvesting of 1.2 L/m^2/day[32]. These lab-scale prototypes suggest that large surface areas ~1000 m^2 would be required to produce even one m^3 of water per day using AWH, and the energy costs are often not considered.

Thermodynamically, both desalination and AWH involve the separation of water from a mixture (salt/water for desalination and air/water for AWH) with some energy input, as shown in Fig. 1a. The reversible energy consumption thus has the same functional form for both processes, with the difference being in the water activity, a_w of saline water versus ambient air. Given that a lower activity corresponds to a larger energy requirement to extract water from the mixture, we find that for ambient air a_w = 0.65 (equivalent to a median global relative humidity of 65%) and for seawater a_w = 0.97 (salinity of 35 g/kg). This simple thermodynamic argument reveals that AWH inherently requires more energy than seawater desalination as water is extracted from a more dilute source.

The interest in AWH for clean water production thus raises important questions about its competitiveness, both in terms of performance and cost. First, what is the energy consumption of AWH at a given location on a kWh/m^3 basis, and how does this compare with distributed desalination (seawater desalination followed by

[a] George W. Woodruff School of Mechanical Engineering, Georgia Institute of Technology, Atlanta, GA, USA
* Corresponding author. Email: akanksha.menon@me.gatech.edu
Electronic Supplementary Information (ESI) available: [details of any supplementary information available should be included here]. See DOI: 10.1039/x0xx00000x

water transport to the same inland location)? Literature reports on AWH energy consumption are limited to thermodynamic analyses of different AWH systems rather than real data under varying operating conditions – for example, Rao *et al*.[24] and Kwan *et al*.[33] evaluated the least work of separation for reversible AWH, and they found that AWH systems operate at a fraction of the reversible limit. Li *et al*.[34] developed models for irreversible (semi-idealized) sorbent AWH in single and multi-stage configurations, and they found that its energy consumption is 67% higher than the enthalpy of vaporization of water. This is an important finding since other processes that rely on evaporative phase change such as thermal desalination are known to be prohibitively expensive and inefficient unless heat recovery is implemented[35,36]. Yet, most AWH prototypes are designed as single-stage devices with low water yields. In the literature, only Kwan *et al*. provided a comparison between reversible AWH and seawater desalination, but their analysis did not consider any location-specific data (weather, population density, water risk, etc.), or make comparisons to distributed desalination to meet inland demand.

Beyond energy consumption, cost is a major driver for the widespread adoption of any technology. AWH is often claimed to be low cost owing to its simple design, minimal infrastructure needs compared to desalination, and the use of low-grade or "free" energy sources[29,31] – however, there is very limited cost data, and the energy consumption of passive systems cannot be neglected as we discuss later. Siegel and Conser[37] estimated the levelized cost of water (LCOW) of a multi-stage liquid desiccant-based AWH system in Southern California to be \$6.5/m^3, but similar analyses on solid sorbents (which is the focus of much research) is lacking. This prompts the second important question: what is the cost of different AWH systems on a \$/m^3 basis, and how does it compare with distributed desalination for locations around the globe? There is thus a significant knowledge gap on the realistic implementation of AWH to address global water stress. Consistent with this, Wang *et al*. recently highlighted the need for the scientific community to critically evaluate the potential of and pathways to improve the performance and cost of AWH[38].

In this work, we present a holistic framework to (i) evaluate the energy consumption of AWH and seawater desalination with inland transport (Fig. 1b) using global weather data[39], population density[40] and water risk[41] data, thereby providing a global map where each approach is best suited from an energy standpoint. The analysis framework is also used to (ii) determine the LCOW of three AWH technologies (Fig. 1c) – dewing from active cooling[42], dewing from passive/radiative cooling[32], and heat-driven sorption systems[26,34] – to pinpoint locations where each would be cost-effective. These results (for practical/irreversible AWH as well as hypothetical reversible AWH systems) are compared to the LCOW of seawater desalination (\$1/m^3), with energy costs added for transporting clean water to different locations inland (using geography data[43] and water transport costs[14]). This comparative analysis is then used to answer two additional questions about AWH: which AWH system has the potential to achieve cost parity with desalination, and what areas of research (materials and system design) should be prioritized to achieve this? Overall, this framework helps establishes cost and performance targets to guide the development of AWH, particularly sorbent technologies, to address global water stress at scale.

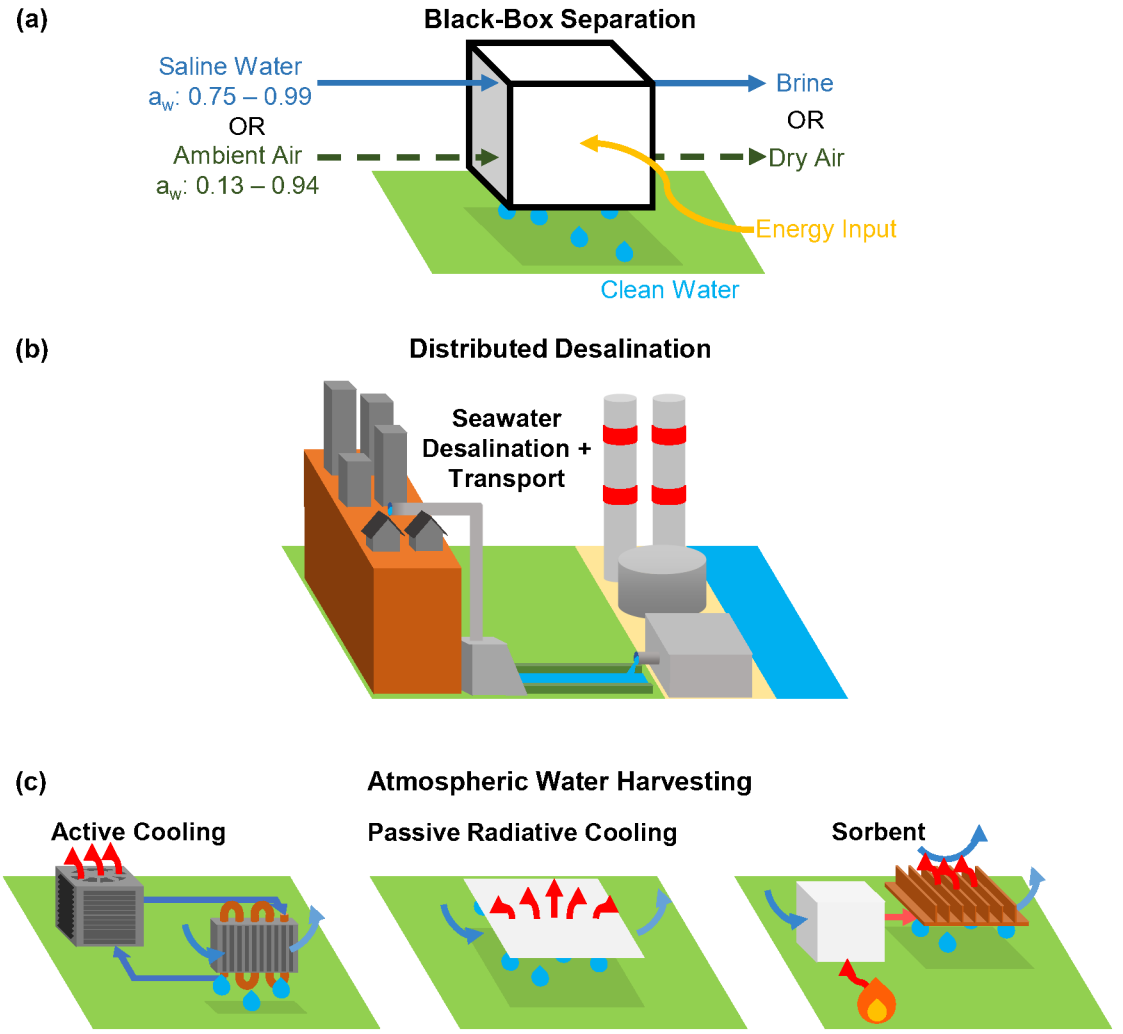

Fig. 1 Desalination and AWH processes analyzed in this work. **(a)** Black-box separator, where water enters as a mixture (saline water or ambient air) and clean water is extracted using some energy input. **(b)** The distributed desalination approach: seawater is desalinated at the coast using reverse osmosis (RO), and the clean water is transported inland using a network of pipes, canals, and tunnels. **c.** Three different atmospheric water harvesting technologies are considered: active cooling (a vapor compression air conditioner cools the air below the dew point to condense water), passive radiative cooling (surface rejects heat to outer space and cools the air below the dew point to condense water), and sorbent systems that desorb moisture (when heat is applied); this humidified air is cooled to ambient temperature to condense water.

Results

Thermodynamic framework for energy consumption

To establish the thermodynamic limits of AWH and desalination, we first derive the least work of separation, W_{min} (the reversible specific energy consumption or SEC), which is a function of the water activity shown in Eq. (1):.

$$W_{min} = -R_w T_{amb} \ln(a_w) \quad (1)$$

where R_w is the specific gas constant of water, T_{amb} is the ambient temperature (K), and a_w is the water activity. For ambient air, a_w is equivalent to the relative humidity, while for saline water it is equal to the product of mole fraction of water and activity coefficient. When the mole fraction of water is high (~0.97 for seawater), the activity coefficient is nearly unity, and the activity of saline water approaches the water mole fraction.

Eq. (1) applies to any internally and/or externally reversible work-driven separation system that produces pure water (Fig. 1a). The energy required for reversible heat-driven separation is equal to this reversible work multiplied by a factor of $\left(1 - \frac{T_{amb}}{T_s}\right)^{-1}$, where T_s is the heat source temperature. In Fig. 2a, we plot the least work of separation as a function of water activity (solid black curve) and indicate the ranges corresponding to ambient air (13 - 94% relative humidity, the lowest and highest annual geometric mean relative humidities across the world) and saline water (brackish water at a salinity of 8.15 g/kg to saturated NaCl at 360 g/kg). The activity of seawater, as well as the median average annual relative humidity values experienced by the global population and the global water risk

weighted (WRW) population are indicated in dashed lines (Methods). Figure 2a shows that half the global population lives in regions where the relative humidity is lower than 68%, which results in an AWH energy consumption ~20 kWh/m^3 even under reversible operation. The higher activity of seawater reduces the reversible energy consumption by 25 × to ~0.8 kWh/m^3. This finding is consistent with of Kwan *et al.*[33] concluding that AWH cannot energetically outperform desalination.

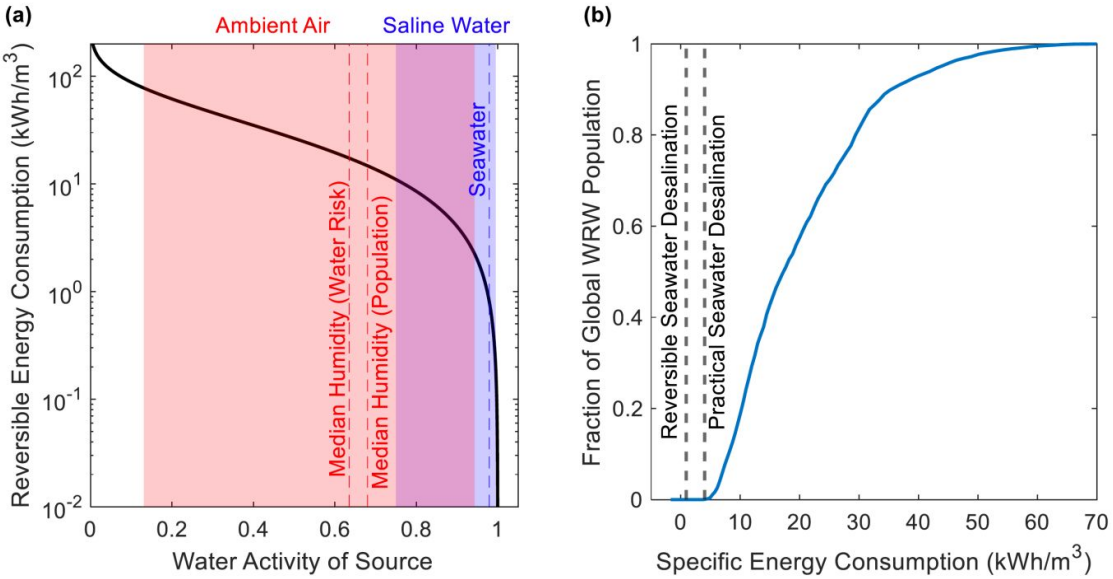

Fig. 2 Thermodynamic limits of freshwater production (least work of separation). **(a)** The reversible specific energy consumption (SEC) of AWH and desalination as a function of water activity for extracting freshwater from ambient air (red shaded region) and saline water (blue shaded region). The global population weighted median relative humidity is approximately 68% and the global water risk weighted median relative humidity is 63.5% (red dashed lines), while the activity of seawater is ~0.97 (blue dashed line). The water risk weighting factor is the product of water risk and population within each grid cell (Methods). **(b)** Cumulative distribution showing the fraction of the water risk weighted (WRW) global population that is in a location where the reversible energy consumption of AWH is below a certain value (shown on the horizontal axis). Vertical dashed lines represent the reversible and practical SEC values for seawater desalination at a salinity of 35 g/kg.

We now put these thermodynamic results in the context of global water stress – Fig. 2b shows a cumulative distribution representing the fraction of the water risk weighted (WRW) population with access to reversible AWH at an energy consumption below the value on the horizontal axis (Methods). This reveals that reversible AWH is more energy intensive than even practical desalination (operational plants have an SEC of 4 kWh/m^3 using reverse osmosis, see Table S1) for 100% of the WRW population. In other words, if seawater (or a saline water source of lower salinity, *e.g.*, brackish water) is available, desalination is always more energetically favorable compared to an AWH system even if it were engineered to be reversible. We note that a comparison with practical AWH is not made because these systems require a phase change of water, resulting in a further increase in energy consumption (latent heat of vaporization is 667 kWh$_{th}$/m^3).

Despite its higher energy footprint, AWH has the advantage of being implemented at any location, while seawater desalination is limited to freshwater production at the coast. However as noted in the introduction, water-stressed regions are combining seawater desalination with clean water transport to meet inland demand. For this scenario, we analyze the energy required to desalinate water at the nearest coast and transport (pump) it to different inland locations, which has not been considered in prior thermodynamic analyses. The energy required for pumping water depends on the vertical and horizontal distance of each location from the nearest coast, which is then added to the SEC of seawater desalination (see Supplementary Note 3). We compare the energy consumption of reversible AWH to that of practical seawater desalination with transport in Fig. 3 to evaluate which approach is more efficient for different locations. The SEC area maps are colored only in locations where each process is more efficient, with AWH systems being more efficient for approximately 40% of the global land area. However, this area corresponds only to 15% of the global WRW population and assumes reversible operation which cannot practically be achieved. We note that Fig. 3 assumes that desalination, water transport, and AWH are all work driven processes. However, sorbent-based AWH (which has been the focus of much research) is typically heat-driven – we find that the overall trends remain the same in this case, with reversible sorbent AWH being more efficient than desalination with transport for only 15-20% of the global WRW population (Supplementary Note 4).

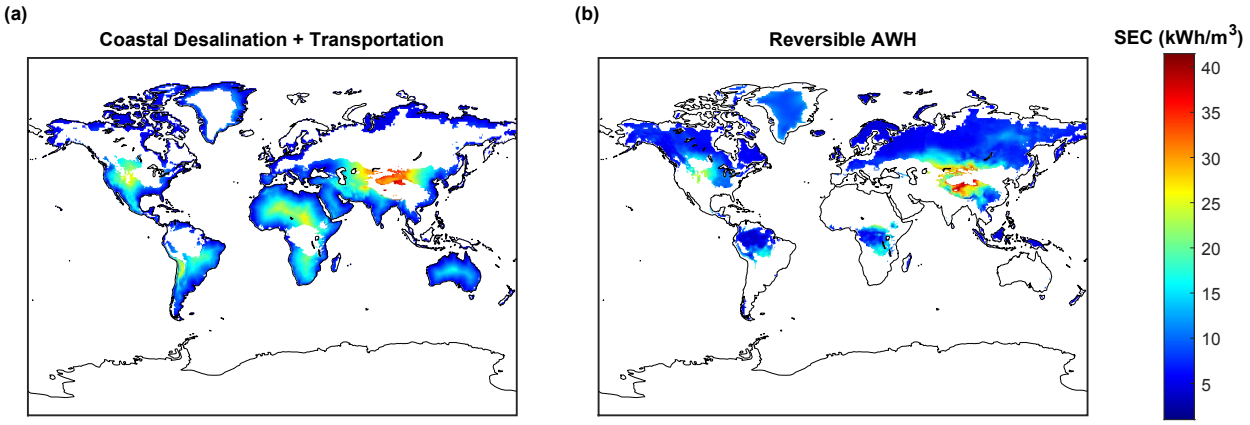

Fig. 3 Maps of the specific energy consumption of practical distributed desalination vs. reversible atmospheric water harvesting for all global locations. Contour plots show the SEC of **(a)** seawater desalination with transport (pumping) of that clean water to inland locations, and **(b)** reversible AWH. The map in (a) is colored only in locations where coastal desalination with transport is more energy efficient than AWH, while the map in (b) is colored where reversible AWH is more efficient.

This energy analysis conclusively shows that AWH for global freshwater production is more energy intensive than desalinating water and transporting it inland even under the most favorable assumptions (*i.e.,* reversible operation). However, such a thermodynamic argument is not sufficient for technology selection where cost is a major driver. In other words, AWH may be able to achieve a lower cost than desalination as it is not infrastructure or capital intensive. Developing cost benchmarks for different types of AWH systems is the focus of the next section given the lack of data in the literature.

Technoeconomic modeling framework for water cost

We first establish the baseline specific costs ($/m^3) for practical AWH systems, *i.e.*, systems that condense water (irreversible operation). Three different AWH technologies are analyzed: active cooling (*i.e.*, a vapor compression refrigeration system that cools air below the dew point to condense water), a passive radiative cooling surface (that radiates heat to space, reaching sub-ambient temperatures to condense water), and a sorbent material (that increases the humidity of the air through desorption) followed by ambient cooling (to condense water). Each AWH technology requires water storage to meet the demand, because freshwater production fluctuates throughout the day with variations in ambient humidity and temperature. A levelized cost of water (LCOW) framework[21] is used to incorporate the lifetime capital and operating expenditures (including the cost of energy) for each technology and levelizing that over the lifetime water production. To find the LCOW of AWH systems in $/m^3, Eq. (2) is used:

$$LCOW = \frac{(CAPEX_i + CAPEX_{WS} \times V_{WS,i}) \times (CRF)}{Yield_i} + C \quad (3)$$

where $CAPEX_i$ is the capital expenditure of the AWH technology (in $ per unit system size), $CAPEX_{WS}$ is the capital expenditure of water storage (in $/m^3 of water storage), $V_{WS,i}$ is the volume of water storage needed for a given AWH technology (in m^3 of water storage per unit system size), CRF is the capital recovery factor or amortization factor, $OPEX_{fix}$ accounts for fixed operations and maintenance costs (in $ per unit system size per year), $Yield_i$ is the annual water produced (in m^3 of water per unit system size per year), and $OPEX_e$ is the variable operating costs associated with energy consumption (in $/m^3 of water produced). The subscript *i* in Eq. (4) corresponds to a particular AWH technology being analyzed (active cooling, passive cooling, or sorbent), with the system size measured in tons of refrigeration, m^2 of radiative cooling surface (assuming a TPX polymethylpentene sheet), and kg of sorbent (assuming MOF-303[30,34]), respectively. All the input costs and other assumptions for this model are provided in Supplementary Note 1 (Table S1).

The $OPEX_e$ term can be calculated as the product of the energy cost (levelized cost of electricity - $LCOE$ in $/kWh for active cooling, or heat - $LCOH$ in $/kWh$_{th}$ for the sorbent) and the specific energy consumption (SEC in kWh/m^3 of water for active cooling and kWh$_{th}$/m^3 of water for the sorbent). We note that sorbent AWH systems in the literature often claim to utilize "free" or "passive" energy sources, such as solar or waste heat[26,29,31]. However, collecting and transferring this low-grade energy to the sorbent material requires equipment (*e.g.,* solar absorber and heat exchangers), which incurs capital cost and must be accounted for as a non-zero LCOH[21,44,45]. Since energy costs vary widely with location, we also perform a sensitivity analysis to understand how different LCOH and LCOE values impact the LCOW, including quantifying what LCOH could be considered "free" as we discuss later (Supplementary Note 5). The radiative cooling system has no energy cost as the surface is incorporated into the capital expenditure term, and the energy consumption of any fans required to blow air is neglected (Supplementary Note 11). The SEC to produce water using each practical AWH system with location specific considerations is derived in Supplementary Notes 6-8. Using this framework and Eq. (5), the LCOW was determined in three representative locations that span the range of climates: Aruba (humid), Niger (dry), and Perth (variable humidity). Even though these LCOW values were calculated for practical AWH operation, some favorable assumptions were made (Supplementary Notes 1, 6-8). The total LCOW and the cost breakdown for each system is shown in Fig. 4.

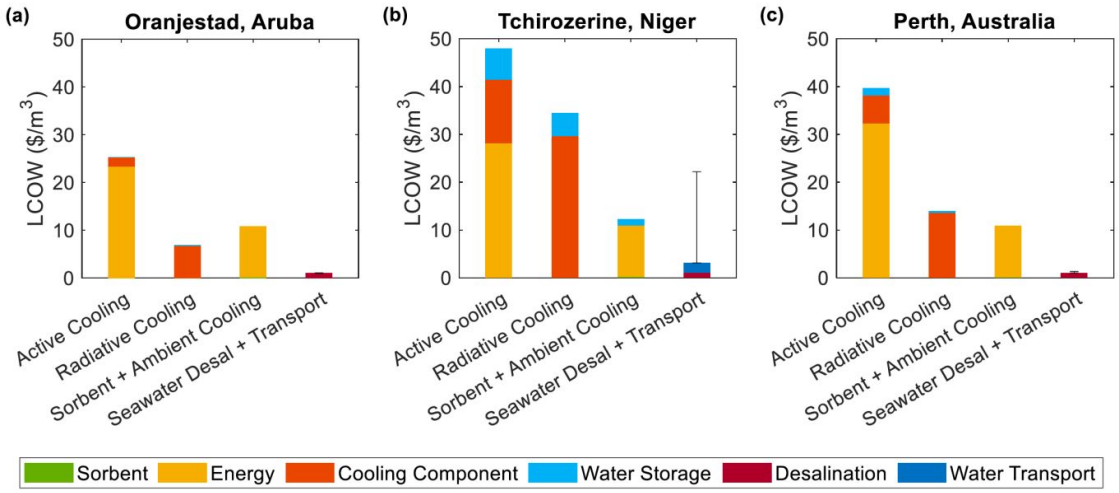

Fig. 4 Cost comparison of three practical AWH technologies with seawater desalination and transport. The LCOW of different AWH technologies in **(a)** Aruba, which has consistently high humidity; **(b)** Niger, which has consistently low humidity; **(c)** Perth, which has highly variable humidity throughout the year. The cooling component is a vapor compression system for active cooling, an ideal radiative cooling surface (TPX polymethylpentene sheet) for passive cooling, and a metal condensing surface for the sorbent (MOF-303) with ambient cooling. The energy consumption is electricity (LCOE) for active cooling and heat (LCOH) for the sorbent. In all three plots, the LCOW of seawater desalination (reverse osmosis) with transport is shown, with the error bars representing 10 × water transport costs (Methods and Supplementary Note 1).

We find that active cooling AWH is hindered by the large energy input required to condense water, resulting in very high LCOW values (> \$20/m^3), even in a humid (favorable for dew harvesting) location shown in Fig. 4a. The passive (radiative cooling) system is less expensive than the active system in all three locations, but the large surface area required to produce one m^3 of water drives up the cost. The passive cooling system is the cheapest AWH option in very humid locations (represented by Aruba) because it benefits from a high dew point. In arid regions and locations with highly variable humidity, the sorbent system has the lowest LCOW among AWH systems as shown in Fig. 4b and Fig. 4c. This can be attributed to three factors - first, the sorbent can absorb moisture from as low as 13% relative humidity (while the active and passive cooling systems are not always able to cool below the dew point without freezing water). Second, the desorption process uses heat, which is cheaper than electricity (making sorbents more suitable to active cooling AWH). Third, the sorbent material (MOF-303) and metal plate required to condense liquid water are assumed to be inexpensive (see Supplementary Notes 1 and 8, respectively). Even though this heat is inexpensive, it is required in large amounts (~1000 kWh$_{th}$ to produce one m^3 of water in all three locations), resulting in the LCOW ranging from 10 – 12 \$/m^3. This is an important finding that is in direct contradiction to literature reports claiming that energy use for sorbent regeneration is "free" or negligible. In most cases the water storage cost is low, except when AWH is unable to produce water for a significant portion of the year. This happens when the air is too dry, preventing the cooling system from condensing water and the sorbent system from absorbing water. To account for this, we considered a range of cut-off relative humidities below which the AWH system is not operated – this prevents the system from operating inefficiently (thus, reducing energy costs), but it also decreases the capacity factor (thus, increasing the cooling component and water storage costs). For each location, the cut-off relative humidity was calculated such that it minimizes the LCOW for each technology by balancing the energy and water storage costs (Supplementary Note 9).

Having established these baseline system costs for practical AWH in representative global locations, we now compare their LCOW to that of seawater desalination at \$1/m^3; this value is based on operational coastal reverse osmosis plants and considers both capital and operating expenditures (including LCOE), as well as the cost of brine disposal (via ocean discharge)[46,47]. To this LCOW for desalinating seawater at the nearest coast (located using MATLAB's built-in Global Self-Consistent Hierarchical High-Resolution Geography data[43]), the cost associated with transporting water inland is added to directly compare AWH and desalination at a given location. We note that the water transport cost is also levelized over the lifetime of the infrastructure, which includes capital and operating expenditures for a combination of pipes, canals, and tunnels[14] (Methods). We find that coastal desalination plus transport is still 4-10 × cheaper than any AWH system in all representative locations, as shown in Fig. 4. Given the variability in water conveyance costs, we analyze an additional scenario where transport costs (both horizontal and vertical) are an order of magnitude higher (represented by error bars in Fig. 4). This reveals a niche that sorbent based AWH can fill cost-effectively: freshwater production in remote and dry locations (Sahara Desert as the representative arid location - Fig. 4b) where no saline water source is available, and where clean water transport costs from the nearest coast are at least 5 × higher than assumed here (see Methods and Supplementary Note 3).

To illustrate global locations where either desalination with transport or sorbent-based AWH is the cost optimal solution, we construct Fig. 5 as a contour plot of the LCOW (colored only in locations where a given method is cheaper, with water transport costs being 5 × the baseline value). We find that the LCOW of AWH is relatively insensitive to location (owing to the low sorbent cost assumed in Table S1), ranging from 10.8 – 12.8 \$/m^3 as shown in Fig. 5b. We note that these values for freshwater production are far too high to be affordable, especially in regions that need it the most.

Furthermore, the land area where sorbent AWH is cheaper corresponds to only 6% of the WRW population as these are remote and arid regions like the Sahara Desert. Even when the desalinated water transport cost is 10× the base value, AWH becomes the more cost-effective option for only 32% of the WRW population (Supplementary Note 10).

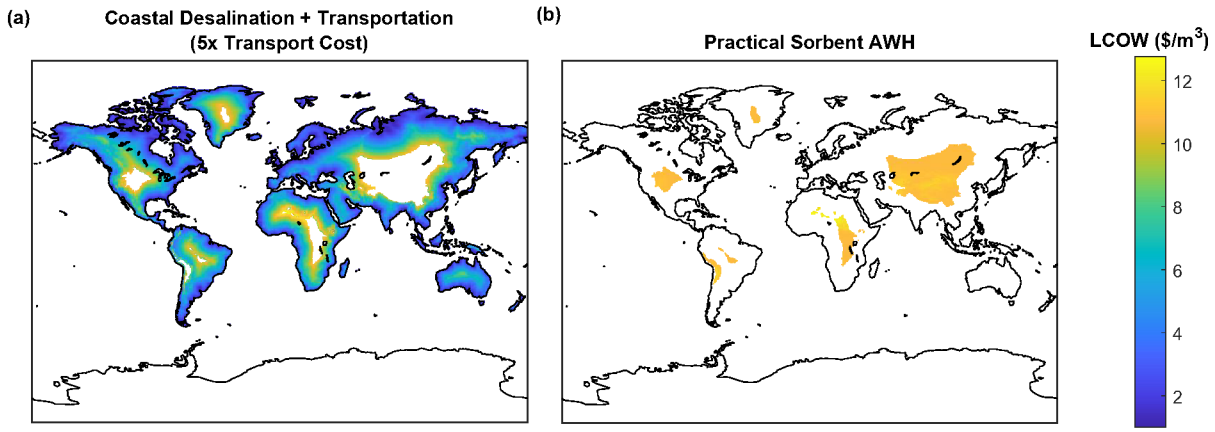

Fig. 5 Maps of LCOW for practical desalination and sorbent-based AWH systems. **(a)** Contour plot showing the LCOW of coastal desalination with water transport, and **(b)** LCOW of practical sorbent AWH. For this figure, a water transport cost 5 × the base value was used (see Methods and Table S1 for base value). The map in (a) is colored only in locations where desalination with transport is cheaper, while the map in (b) is colored in locations where sorbent AWH is cheaper.

Given that energy consumption is a major contributor to the AWH cost, we consider a hypothetical scenario in which the system operates reversibly to establish the minimum possible LCOW. This means that the AWH system can produce significantly more water for the same size (refrigeration tonnage for active AWH, radiative cooling surface area, or sorbent mass) and energy input without incurring any increase in capital expenditure. Again, the cut-off relative humidity and maximum hourly water yield were optimized to find the lowest LCOW at each location. The results are presented in Fig. 6 as a cumulative distribution representing the fraction of the WRW population with an LCOW ratio (reversible AWH to practical distributed desalination) shown on the horizontal axis. When this ratio is less than unity (green shaded region), reversible AWH is more cost effective; when the ratio is greater than unity (red shaded region), practical seawater desalination with transport (assuming baseline water transport costs) is preferred from a cost standpoint. This distribution reveals a promising outcome for AWH – reversible sorbent systems can be cheaper than distributed desalination for ~95% of the global population, while reversible active and passive cooling AWH systems would be cheaper for only ~33% and 5% of the WRW population, respectively. Although these AWH system costs are unrealistic given the reversible assumption, they provide the best-case scenario that can be achieved by reducing energy consumption. In the following section, we outline the research opportunities that can help reduce the energy footprint and cost of AWH systems.

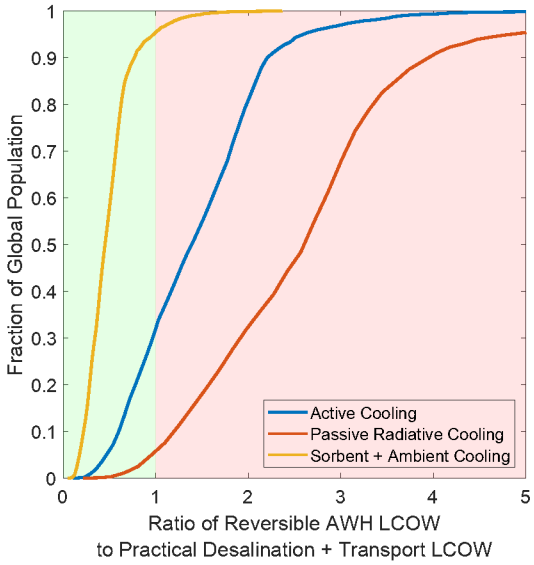

Fig. 6 Levelized water cost comparison (cumulative distribution) of three different reversible AWH technologies to practical desalination with transport (baseline value). The vertical axis represents the fraction of the global WRW population with an LCOW ratio equal to or less than the value on the horizontal axis.

Opportunities for AWH cost reduction

The thermodynamic and technoeconomic analysis has shown that among the AWH technologies, sorption-based systems are most promising. However, these systems must significantly reduce their energy footprint to drive down their LCOW. Practical approaches to reduce energy consumption include a system design that recuperates latent heat (*i.e.,* multi-stage operation[31]). This would however incur a significant increase in capital cost due to the heat exchangers required for multi-stage operation. Furthermore, increasing the number of stages beyond a certain point has diminishing returns, yielding only a small increase in energy efficiency for a sizeable increase in cost. Another approach to reduce the LCOW is by using a low-cost heat source (*i.e.,* lower LCOH). In our analysis of the practical sorbent AWH system, a regeneration temperature of 135 °C was assumed as it yields the lowest specific energy consumption for single-stage sorbent AWH[34]. However, at a regeneration temperature of 80 °C, the SEC is only 37% higher, indicating that there is an optimal regeneration temperature which balances the cost of heat (increases with temperature[44,48]) and energy consumption for desorption (decreases with temperature till the optimal regeneration value). To evaluate the impact of LCOH and regeneration temperature on LCOW, a sensitivity analysis is performed (Supplementary Note 5). We find that even a significant decrease in LCOH to 0.1 ¢/kWh$_{th}$ would lower LCOW to \$2.93/m^3 and \$2.53/m^3 at regeneration temperatures of 80 °C and 135 °C, respectively; this would approach cost parity with desalination plus transport to a remote location. While it may seem that lower regeneration temperatures can reduce the LCOW further, we note that SEC increases rapidly at temperatures below 80 °C[34], suggesting that the integration of low-grade heat sources is not worthwhile. We also show that the energy can only be considered "free" or negligible (*i.e.*, energy cost contributes less than \$0.1/m^3 to the total LCOW) if the LCOH is below 0.01 ¢/kWh$_{th}$ (Supplementary Note 5). This is unrealistically low and reveals that energy will be the bottleneck for any practical implementation of sorbent-based AWH.

Beyond these system-level targets, the framework also reveals what material properties can lower the LCOW. Specifically, a low specific heat for the sorbent is desirable, as a high specific heat increases energy consumption beyond the reversible limit. The sorption isotherm inflection point should also be selected based on the ambient conditions of the location where the AWH system will be used – specifically, this inflection point should correspond to a value near the lowest relative humidity experienced during the year to maximize the number of hours that the sorbent can absorb moisture from air. However, the inflection relative humidity should not be too low, as this increases SEC. For example, in Aruba, (the representative humid location), the relative humidity never dips below 43%, so the isotherm inflection point should be close to this value. Overall, a careful balance of the capacity factor (fraction of the year during which the sorbent can absorb moisture), energy consumption, and sorption kinetics should be considered for optimizing the sorption isotherm for a particular location. The desorption enthalpy will also likely play an important role in minimizing LCOW as it affects the energy consumption – Li *et al.*[34] showed that the energy consumption in a dual-stage sorbent system decreased by nearly 40% when the desorption enthalpy changed from that of MOF-303 at 2900 kJ/kg, to an optimal value of 3500 kJ/kg. It is worth noting, however, that even with the optimal desorption enthalpy, our framework predicts that the system considered by Li *et al.* would still have an LCOW greater than \$6/m^3. The final parameter of interest is the cost of the sorbent (in \$ per kg sorbent) divided by the water uptake of the sorbent (in kg water per kg sorbent). We find that if this value is less than \$8.70 per kg water, the sorbent capital cost contributes less than \$0.1/m^3 to the LCOW (Supplementary Note 2) – this is the cost target that we establish for MOFs and other sorbent materials (at scale synthesis costs have not been reported in the literature). While the optimization of these material properties is important for sorbent AWH, reaching cost parity with desalination or becoming a viable option to address water stress requires commensurate reductions in the energy consumption and/or lower costs of heat as discussed.

Finally, we note that desalination of inland saline sources such as brackish water can be another distributed treatment approach instead of transporting desalinated seawater from the nearest coast. For inland desalination, the cost of brine management must be considered since ocean discharge is not an option, and zero liquid discharge (ZLD) is often the optimal choice[21]. Thus, inland desalination could be a favorable alternative to coastal desalination, provided a saline water source is present and the cost of ZLD is less than the cost of water transport from the coast. Given the nascency of such systems and lack of cost data, they are not considered in the present technoeconomic analysis.

Conclusions

This study presents a holistic evaluation of the energy consumption (thermodynamics) and cost (technoeconomics) of atmospheric water harvesting and desalination as two methods of freshwater production. With the goal of addressing water stress, we use population and water risk data for all global locations to evaluate where each technology (seawater desalination with water transport vs. AWH – active cooling, passive/radiative cooling, sorbent-based) is practically viable. The key findings are:

- The median global water activity of atmospheric air (*i.e.*, relative humidity) is 0.65, whereas the activity of seawater is 0.97 owing to which reversible AWH requires approximately 25 × higher energy consumption than reversible desalination.
- Even practical (irreversible) seawater desalination at the coast with transport of this clean water to inland locations is more energy-efficient than reversible AWH for almost 90% of the global water risk-weighted population. Practical AWH systems would require significantly more energy owing to the enthalpy of condensation to produce liquid water, which is significantly higher than the reversible energy requirement (667 kWh$_{th}$/m^3 for condensation vs. 14 kWh/m^3 for reversible separation at a relative humidity of 70%).
- Evaluation of the AWH costs on a levelized basis shows that passive radiative cooling systems achieve the lowest LCOW among the AWH systems in humid locations, but this cost is still approximately 6 × higher than the cost of seawater desalination (reverse osmosis) with transport.
- In locations that are dry or have highly variable humidity, sorbent-based AWH systems achieve lower LCOWs than the active and passive cooling systems, but this cost of ~\$11/m^3 is still prohibitively high for realistic implementation.
- The niche that sorbent-based AWH can fulfill is when water conveyance costs are high and the location is far from the coast (*e.g.,* Sahara Desert). Furthermore, reversible operation is unrealistic as the reduction in energy consumption would require large and thus expensive surfaces for heat and mass transfer.

- Material and system-level design modifications are required for sorbent-based AWH to approach cost parity with desalination. Specifically, the cost of heat (LCOH) would have to decrease by at least an order of magnitude to 0.1¢/kWh_{th} and the sorbent material itself should cost less than $8.70 per kg water.

Methods

Average Annual Relative Humidity

For the thermodynamic analysis, the average annual relative humidity for each location across the globe was calculated to estimate the average energy input accurately. For this, we used relative humidity data from NASA's MERRA 2 dataset[39] (which contains relative humidity data for each hour of the year in grid cells that span the globe). Because the least work of separation expression contains the natural logarithm of relative humidity, it is important to calculate the geometric mean of relative humidity, not the arithmetic mean. Then, the yearly geometric mean relative humidity and arithmetic mean temperature can be used to find the average annual least work of separation for a given location. It should be noted that using the geometric mean relative humidity and arithmetic mean temperature is an approximation, but it produces results with minimal error while significantly reducing computational time.

Weather, Population, and Water Risk Data

For weather (temperature and humidity) data, we used NASA's MERRA 2 dataset[39], which provides hourly temperature and humidity data within a 722 × 362 grid of the Earth's surface. This dataset was used for the thermodynamic analyses (Fig. 2 and Fig. 3) and cost analyses (Fig. 4, Fig. 5, and Fig. 6). We weighted our results by two factors: population density and the product of population with water risk. For this, gridded datasets for population[40] and water risk[41] were obtained to find the population and water risk within each cell of the 722 × 362 grid. For the specific locations analyzed in Fig. 4, TMYx data[49] was used.

Cumulative Distribution of the Specific Energy Consumption for Reversible AWH

To calculate the cumulative distribution in Fig. 2b, we calculated the reversible SEC of AWH using Eq. (1) for each grid cell of the Earth's surface, with the abovementioned NASA MERRA 2 dataset. We then used this data, along with data of the global WRW population within each grid cell, to calculate the fraction of the global WRW population that resides in a location where the reversible AWH SEC was below a particular value shown on the horizontal axis. The same general approach was used to obtain the cumulative distribution plot in Fig. 6 (but with the horizontal axis showing relative reversible LCOW instead of reversible SEC).

Water Transportation Costs

For water transportation costs, we reference the work by Zhou and Tol[14], who performed a review of vertical and horizontal water transportation costs from various literature sources. They show a cost of \$5 × 10^{-4} per m^3 water per m of vertical distance transported, and we use this vertical transport cost in our analysis. They also provide a cost of \$6 × 10^{-4} per m^3 water per km of horizontal distance transported, which they state corresponds to canals, tunnels (108% more expensive than canals), and pipes (which are 271% more expensive than canals). Using this information, we assume an equal mix of canals, tunnels, and pipes, which results in a cost of \$13.58 × 10^{-4} per m^3 water per km of horizontal distance transported. It should be noted that using a mix of canals, tunnels, and pipes is common as evidenced by the Colorado River Aqueduct[50]. These horizontal and vertical costs were also increased by an order of magnitude to understand its impact on LCOW (\$5 × 10^{-3} per m^3 water per m of vertical distance and \$13.58 × 10^{-3} per m^3 water per km of horizontal distance for the high-cost scenario).

Author Contributions

Conceptualization: JDK, AKM
Methodology: JDK, AKM
Investigation: JDK
Visualization: JDK
Project administration: AKM
Supervision: AKM
Writing – original draft: JDK
Writing – review & editing: JDK, AKM

Conflicts of interest

There are no conflicts to declare.

Acknowledgements

J.D.K. acknowledges financial support from the IBUILD Fellowship. This research was performed under an appointment to the Building Technologies Office (BTO) IBUILD-Graduate Research Fellowship administered by the Oak Ridge Institute for Science and Education (ORISE) and managed by Oak Ridge National Laboratory (ORNL) for the U.S. Department of Energy (DOE). ORISE is managed by Oak Ridge Associated Universities (ORAU). All opinions expressed in this paper are the author's and do not necessarily reflect the policies and views of DOE, EERE, BTO, ORISE, ORAU or ORNL.

Notes and references

1 *Global risks 2019: insight report*, World Economic Forum, Geneva, 14th Edition., 2019.
2 H. Ritchie and M. Roser, *Our World in Data*.
3 Water Scarcity, https://www.unwater.org/water-facts/water-scarcity, (accessed February 9, 2023).
4 C. J. Vörösmarty, P. B. McIntyre, M. O. Gessner, D. Dudgeon, A. Prusevich, P. Green, S. Glidden, S. E. Bunn, C. A. Sullivan, C. R. Liermann and P. M. Davies, *Nature*, 2010, **467**, 555–561.
5 L. Schleifer, .
6 Y. J. Lim, K. Goh, M. Kurihara and R. Wang, *Journal of Membrane Science*, 2021, **629**, 119292.
7 M. Elimelech and W. A. Phillip, *Science*, 2011, **333**, 712–717.
8 J. Eke, A. Yusuf, A. Giwa and A. Sodiq, *Desalination*, 2020, **495**, 114633.
9 E. Jones, M. Qadir, M. T. H. van Vliet, V. Smakhtin and S. Kang, *Science of The Total Environment*, 2019, **657**, 1343–1356.
10 Water | The Official Portal of the UAE Government, https://u.ae/en/information-and-services/environment-and-energy/water-and-energy/water-, (accessed August 3, 2023).
11 UAE, https://www.statista.com/statistics/745140/uae-desalination-water-plants-capacity/, (accessed August 3, 2023).
12 A. C. W. DC, The Costs and Benefits of Water Desalination in the

Gulf, https://arabcenterdc.org/resource/the-costs-and-benefits-of-water-desalination-in-the-gulf/, (accessed August 3, 2023).
13 Factsheet: People and Oceans, https://www.un.org/sustainabledevelopment/wp-content/uploads/2017/05/Ocean-fact-sheet-package.pdf.
14 Y. Zhou and R. S. J. Tol, *Water Resources Research*, , DOI:10.1029/2004WR003749.
15 J. Partlow, *Washington Post*, 2022.
16 B. Walton, Australia Builds Desalination Plants and Pipelines to Bring Water to Mines, https://www.circleofblue.org/2011/world/australia-builds-desalination-plants-and-pipelines-to-bring-water-to-mines/, (accessed August 1, 2023).
17 Z. H. Foo, C. Stetson, E. Dach, A. Deshmukh, H. Lee, A. K. Menon, R. Prasher, N. Y. Yip, J. H. Lienhard and A. D. Wilson, *Trends in Chemistry*, 2022, **4**, 1078–1093.
18 C. T. K. Finnerty, A. K. Menon, K. M. Conway, D. Lee, M. Nelson, J. J. Urban, D. Sedlak and B. Mi, *Environ. Sci. Technol.*, 2021, **55**, 15435–15445.
19 A. Z. Haddad, A. K. Menon, H. Kang, J. J. Urban, R. S. Prasher and R. Kostecki, *Environ. Sci. Technol.*, 2021, **55**, 3260–3269.
20 A. K. Menon, I. Haechler, S. Kaur, S. Lubner and R. S. Prasher, *Nat Sustain*, 2020, **3**, 144–151.
21 A. K. Menon, M. Jia, S. Kaur, C. Dames and R. S. Prasher, *iScience*, 2023, **26**, 105966.
22 M. S. Mauter and P. S. Fiske, *Energy Environ. Sci.*, 2020, **13**, 3180–3184.
23 G. Chen, *Phys. Chem. Chem. Phys.*, 2022, **24**, 12329–12345.
24 A. K. Rao, A. J. Fix, Y. C. Yang and D. M. Warsinger, *Energy Environ. Sci.*, , DOI:10.1039/D2EE01071B.
25 F. Zhao, X. Zhou, Y. Liu, Y. Shi, Y. Dai and G. Yu, *Advanced Materials*, 2019, **31**, 1806446.
26 H. Kim, S. R. Rao, E. A. Kapustin, L. Zhao, S. Yang, O. M. Yaghi and E. N. Wang, *Nat Commun*, 2018, **9**, 1191.
27 T. Li, M. Wu, J. Xu, R. Du, T. Yan, P. Wang, Z. Bai, R. Wang and S. Wang, *Nat Commun*, 2022, **13**, 6771.
28 Y. Zhang, W. Zhu, C. Zhang, J. Peoples, X. Li, A. L. Felicelli, X. Shan, D. M. Warsinger, T. Borca-Tasciuc, X. Ruan and T. Li, *Nano Lett.*, 2022, **22**, 2618–2626.
29 J. Lord, A. Thomas, N. Treat, M. Forkin, R. Bain, P. Dulac, C. H. Behroozi, T. Mamutov, J. Fongheiser, N. Kobilansky, S. Washburn, C. Truesdell, C. Lee and P. H. Schmaelzle, *Nature*, 2021, **598**, 611–617.
30 Z. Zheng, H. L. Nguyen, N. Hanikel, K. K.-Y. Li, Z. Zhou, T. Ma and O. M. Yaghi, *Nat Protoc*, 2022, 1–21.
31 A. LaPotin, Y. Zhong, L. Zhang, L. Zhao, A. Leroy, H. Kim, S. R. Rao and E. N. Wang, *Joule*, 2021, **5**, 166–182.
32 I. Haechler, H. Park, G. Schnoering, T. Gulich, M. Rohner, A. Tripathy, A. Milionis, T. M. Schutzius and D. Poulikakos, *Science Advances*, 2021, **7**, eabf3978.
33 T. H. Kwan, S. Yuan, Y. Shen and G. Pei, *Energy Reports*, 2022, **8**, 10072–10087.
34 A. C. Li, L. Zhang, Y. Zhong, X. Li, B. El Fil, P. F. Fulvio, K. S. Walton and E. N. Wang, *Appl. Phys. Lett.*, 2022, **121**, 164102.
35 *Reducing the Greenhouse Gas Emissions of Water and Sanitation Services: Overview of emissions and their potential reduction illustrated by utility know-how*, IWA Publishing, 2022.
36 J. Swaminathan, H. W. Chung, D. M. Warsinger and J. H. Lienhard V, *Applied Energy*, 2018, **211**, 715–734.
37 N. P. Siegel and B. Conser, *Journal of Energy Resources Technology*, , DOI:10.1115/1.4049286.
38 J. Wang, L. Hua, C. Li and R. Wang, *Energy Environ. Sci.*, 2022, **15**, 4867–4871.
39 MERRA-2 tavg1_2d_slv_Nx: 2d,1-Hourly,Time-Averaged,Single-Level,Assimilation,Single-Level Diagnostics V5.12.4 (M2T1NXSLV), https://disc.gsfc.nasa.gov/datasets/M2T1NXSLV_5.12.4/summary.
40 Center For International Earth Science Information Network-CIESIN-Columbia University, 2018.
41 Aqueduct Water Risk Atlas, https://www.wri.org/applications/aqueduct/water-risk-atlas, (accessed December 1, 2022).
42 R. Tu and Y. Hwang, *Energy Conversion and Management*, 2019, **198**, 111811.
43 Read Global Self-Consistent Hierarchical High-Resolution Geography (GSHHG) data - MATLAB gshhs, https://www.mathworks.com/help/map/ref/gshhs.html, (accessed August 2, 2023).
44 T. Gilbert, A. K. Menon, C. Dames and R. Prasher, *Joule*, 2023, **7**, 128–149.
45 C. Geffroy, D. Lilley, P. S. Parez and R. Prasher, *Joule*, 2021, **5**, 3080–3096.
46 I. Baniasad Askari and M. Ameri, *Applied Thermal Engineering*, 2021, **185**, 116323.
47 A. S. Reimers and M. E. Webber, *Texas Water Journal*, 2018, **9**, 82–95.
48 R. Gabbrielli, P. Castrataro, F. Del Medico, M. Di Palo and B. Lenzo, *Energy Procedia*, 2014, **49**, 1340–1349.
49 Repository of free climate data for building performance simulation, https://climate.onebuilding.org/, (accessed January 7, 2023).
50 MWD | Colorado River Aqueduct, https://www.mwdh2o.com/colorado-river-aqueduct-map, (accessed March 1, 2023).